Indian Journal of Pure & Applied Physics
Vol. 57, November 2019, pp. 822-835

Experimental (FT–IR, FT–Raman, and UV–Vis) and quantum chemical calculations on monomer and dimer structures of l-hydroxy-2-naphthoic acid using the DFT and TD–DFT methods

A Eşme*

[a]Department of Elementary Science Education, Education Faculty, Kocaeli University, Umuttepe, Kocaeli 41380, Turkey

Received 8 June, 2018; accepted 6 July 2019

The fourier transform infrared (FT–IR) and fourier transform Raman (FT–Raman) spectra of l-hydroxy-2-naphthoic acid (1H2NA) in solid phase have been experimentally recorded and analyzed in the region 4000–400 cm^{-1}. DFT/B3LYP/6–31G (d,p) calculations were used to determine the optimized molecular structure, conformational, non-linear optical (NLO), natural bond orbital (NBO) analysis, molecular surfaces, Mulliken, NBO charges and vibrational studies of 1H2NA. Obtained results on the geometric structure, vibrational frequencies and UV–Vis spectral analysis are compared with the observed data. The dimeric structure of 1H2NA with the DFT/B3LYP/6–31G (d,p) level caused by the shifts of O–H and C=O bands in the vibrational spectra were also studied. Moreover, the spectroscopic and theoretical results were compared with the corresponding properties for monomeric and dimeric structures of 1H2NA. The detailed vibrational assignments were performed with the DFT calculation, and the potential energy distribution (PED) was obtained by the vibrational energy distribution analysis (VEDA4) program. TD–DFT/B3LYP/6–31G (d,p) calculations with the SCF (self–consistent field) in gas phase and ethanol solvent in the excited state were employed to investigated UV–Vis absorption spectra and the major contributions to the electronic transitions were obtained. The NLO properties such as mean polarizability (<α>), the anisotropy of the polarizability (<$\Delta\alpha$>) and the mean first–order hyperpolarizability (<β>) were computed by using finite field method. The computed values of μ, α and β of the title molecule are 2.2744 D, 17.3225 × 10^{-24} esu and 4.222 × 10^{-30} esu, respectively. The high β values and non-zero values of μ indicate that the title compound might be a good candidate for NLO material.

Keywords: l-hydroxy-2-naphthoic acid, NLO, PED, UV–Vis analysis, FT-IR, FT-Raman

1 Introduction

l-hydroxy-2-naphthoic acid (1H2NA) with bicyclic structure consisting of two benzene rings fused together (Fig. 1) is an aromatic compound mainly used in the production of metallizableazo dye[1], cyan dye[2], napthalide indicator dye[3] and photosensitive substances[4]. In general, napthoic acids are involved in the metabolism of polycyclic aromatic hydrocarbons. Vibrational spectroscopy is used extensively in organic chemistry for the identification of functional groups of organic compounds for studies on molecular conformation, reaction kinetics[5], etc. However, for a proper understanding of FT-IR and Raman spectra, reliable assignments of all vibrational bands are essential. Recently, computational methods based on density functional theory are becoming widely used. This method predicts relatively accurate molecular structure and vibrational spectra with moderate computational effort.

The crystal structure of 1H2NA was re-prepared and re-determined by single–crystal X–ray diffraction method by Q Zhang[6]. To our knowledge, the vibrational (FT–Raman, FT–IR) spectra, UV–Vis analysis and the quantum chemical calculations for

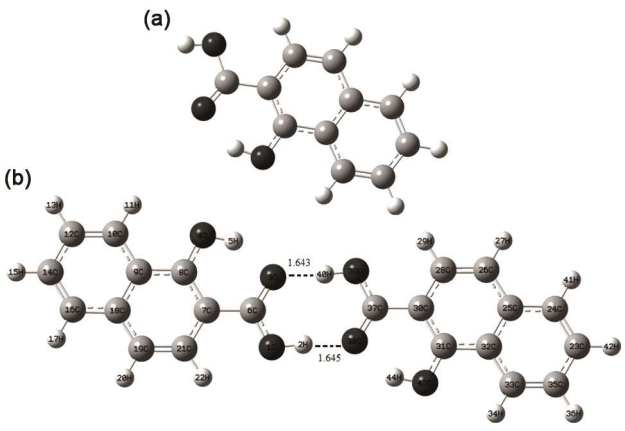

Fig. 1 – The optimized molecular structures (a) monomeric and (b) dimeric forms of 1H2NA obtained from the DFT/B3LYP/6–31G(d,p) level.

(E-mail: asliesme@gmail.com)

this molecule have not been reported so far. Quantum chemical calculations are excellent methods in the design of nonlinear optical (NLO) molecules and help to predict some properties of the new materials, such as molecular dipole moments, polarizabilities and hyperpolarizabilities. The objective of the present study was to provide a complete description of the molecule geometry and vibrational spectra of studied molecule. The present work deals with DFT/B3LYP computations and vibrational spectral analysis of the 1H2NA on the basis of the calculated potential energy distribution (PED). Hence, we characterized the molecular structure, NLO, NBO analysis, vibrational frequencies and molecular electrostatic potential (MEP) map of the title molecule in the ground state and also calculated at the DFT/B3LYP level with the 6–31G (d,p) basis set. DFT/B3LYP/6–31G (d,p) calculation of 1H2NA dimer was performed to support the molecular structure and wavenumber assignments. The total energy HOMO and LUMO energies, the $\Delta E_{\text{LUMO–HOMO}}$ energy gap and global reactivity descriptors like global hardness (η), global softness (σ), chemical potential (Pi) and electrophilicity index (ω) calculations in solvent and gas phase were computed by using TD–DFT/B3LYP/6–31G (d,p) method.

2 Experimental Details

The compound 1H2NA in the solid form was procured from the Sigma–aldrich chemical company (USA) and it was used as such to record FT–IR and FT–Raman spectra. The fourier transform infrared (FT–IR) spectrum of solid studied molecule was recorded using a Agilent Cary 630 FTIR spectrometer equipped with a KBr beam splitter in the region 4000–400 cm^{-1}. The fourier transform Raman (FT–Raman) spectra of the solid title molecule were taken using a nicolet NXR FT–Raman spectrophotometer using a 1064 nm line of a Nd:YAG laser source as the excitation source in the region 4000–0 cm^{-1}. On the other hand the ultraviolet visible spectrum of the title compound was recorded on a dual beam at ambient temperature on a model T80 + UV–vis spectrophotometer using quartz cuvettes with a 1 cm path length.

3 Computational Details

All calculations were performed using the Gaussian 09 Rev A 11.4 package program[7], and the obtained results were visualized by the Gauss View Rev 5.0.9 software[8]. The molecular structure of 1H2NA monomer in the ground state was geometry optimized using the density functional theory (DFT) and the hybrid functional B3LYP. B3LYP is composed of the Becke's three parameter exchange functional (B3) and the nonlocal correlation functional by Lee–Yang–Parr (LYP)[9,10]. The basis set used for all atoms was 6-31G (d,p) in both the DFT and time-dependent density functional theory (TD-DFT) methods.

Moreover, the molecular structure of 1H2NA as a dimer was studied by using the DFT/B3LYP/6–31G (d,p) method. Detailed assignments of vibrational modes were carried out based on percentage potential energy distribution (PED) analysis using the VEDA4 program written by Jamroz[11]. The optimized structure of the title molecule is confirmed to be located at the local true minima on the potential energy surface, as they have not got any imaginary frequency modes.

In the context of the HF theorem, the highest occupied molecular orbital (E_{HOMO}) and the lowest unoccupied molecular orbital (E_{LUMO}) energies are used to approximate the ionization potential (I) and electron affinity (A) given by Koopmans' theorem[12], respectively. The ionization potential ($I = -E_{\text{HOMO}}$) is directly proportional to the HOMO energy and the electron affinity ($A = -E_{\text{LUMO}}$) is directly proportional to the LUMO energy. Using the HOMO and LUMO energies, global chemical reactivity descriptors such as global hardness (η), global softness (σ) and chemical potential (Pi) were carried out. The global hardness $\eta = (I - A)/2 = -\left(E_{HOMO} - E_{LUMO}\right)/2$ is a measure the resistance of an atom to charge transfer[13]. The global softness, $\sigma = 1/\eta = -2/\left(E_{HOMO} - E_{LUMO}\right)$ describes the capacity of an atom or a group of atoms to receive electrons[13]. The chemical potential $Pi = -(I + A)/2 = \left(E_{HOMO} + E_{LUMO}\right)/2$ measures the escaping tendency of an electron from an equilibrium system[14]. Parr *et al.*[15] have defined a new descriptor to quantify the global electrophilic power of a molecule as electrophilicity index (ω), which can be denoted by the formula as follows:

$$\omega = Pi^2 / 2\eta \quad \ldots (1)$$

The ground state dipole moment (μ), the mean polarizability $\langle\alpha\rangle$, the anisotropy of the polarizability $\langle\Delta\alpha\rangle$ and the mean first–order hyperpolarizability (β), using the x, y, z components[16,17] they are defined as:

$$\mu = \left(\mu_x^2 + \mu_y^2 + \mu_z^2\right)^{1/2} \quad \ldots (3)$$

$$\langle \alpha \rangle = \frac{\alpha_{xx} + \alpha_{yy} + \alpha_{zz}}{3} . \quad \ldots (4)$$

$$\langle \Delta\alpha \rangle = \left[\frac{(\alpha_{xx} - \alpha_{yy})^2 + (\alpha_{yy} - \alpha_{zz})^2 + (\alpha_{zz} - \alpha_{xx})^2 + 6(\alpha_{xy}^2 + \alpha_{xz}^2 + \alpha_{yz}^2)}{2} \right]^{1/2} \quad \ldots (5)$$

$$\beta = \sqrt{(\beta_{xxx} + \beta_{xyy} + \beta_{xzz})^2 + (\beta_{yyy} + \beta_{yzz} + \beta_{yxx})^2 + (\beta_{zzz} + \beta_{zxx} + \beta_{zyy})^2} \quad \ldots (6)$$

Because the values of the polarizabilities (<α> and <$\Delta\alpha$>) and the first-order hyperpolarizability (β) of Gaussian 09 Rev A 11.4 program[7] are reported in atomic units (a.u.), the calculated values have been converted into electrostatic units (esu) (α: 1 a.u. = 0.1482×10^{-24} esu; β: 1 a.u. = 8.6393×10^{-33} esu)[18].

4 Results and Discussion

4.1 Structural analysis

The crystal structure of 1H2NA [$C_{11}H_8O_3$] was taken from the Cambridge crystallographic data center (CCDC 1036606). The molecule crystallizes in the monoclinic systems with the space group is *C2/c*. The crystal structure parameters of the studied compound[6] are found to be a = 20.920(5) Å, b = 6.9926(14) Å, c = 14.688(3) Å and V = 1752.7(6) Å^3. Due to the fact that the structure of this molecule has been previously reported in the literature[6], we first investigated this molecule as monomer and dimer forms. The optimize molecular structures along with numbering of the atoms of 1H2NA monomer and dimer forms which contain two intermolecular and two intramolecular hydrogen bonds obtained from the B3LYP/6–31G (d,p) method are shown in Fig. 1 (a and b), respectively. The optimized structural parameters (bond lengths, bond angles and dihedral angles) at the B3LYP/6–31G (d,p) method for 1H2NA monomer are compared with the experimental results[6] and are presented in Table 1.

The optimize bond lengths of C–H lies in the range 1.084–1.087 Å using the DFT/B3LYP level. The experimental values of C–H are found to be almost 0.930 Å, which are smaller than those of the theoretical values using the DFT/B3LYP level while the remaining bond lengths are longer.

The $C_{naphthoic}$–$C_{carboxyliacid}$ (C7–C6) bond length calculated at 1.459Å for the DFT/B3LYP method is shorter than the reported structural data[19] computed by the same method. In international tables for crystallography[20], the C–O bond lengths in the carboxylic acid group conforming to the average values are tabulated for an aromatic carboxylic acid in which C=O is 1.266(20) Å and C–O is 1.305(20) Å. In this study, the corresponding bond lengths in the naphthoic acid are found at 1.243(3) and 1.321(2) Å [6], which are calculated as 1.237 and 1.348 Å by the DFT/B3LYP/6–31G (d,p) method. The calculated C=O and C–O bond lengths in the carboxylic acid show good agreement with literature[5,21].

The O1–H2 and O4–H5 bond distances were found at 0.94(5) and 0.87(4) Å[6] and the lengths were calculated to be 0.972 and 0.992 Å using the DFT/B3LYP level, respectively. The calculated O1–H2 and O4–H5 bond distances are very small compare than other bond lengths but it is excellent agreement with the experimental result. Hence, the O1 and O4 act as lone pair donor.

Secondly, molecular geometric parameter of purposed 1H2NA dimer was also investigated by using the DFT/B3LYP/6–31G (d,p) level Fig. 1(b). The molecules are linked by short intermolecular and asymmetric O–H···O hydrogen bonds between oxygen atom and hydroxyl group of another molecule to give rise to a dimer. The optimized bond lengths, bond angles and dihedral angles for dimer form are also presented in Table 1. The intermolecular hydrogen bonding parameters that are H2···O38, O3··· O39, and O39–H40···O3 are calculated as 1.645 Å, 2.646 Å and 177.915º, respectively. These angles and lengths have calculated[22] at 179.6º, 178.2º and 2.674, 2.670 Å. The calculated molecular geometric parameters for carboxyl group in the title molecule are in good agreement with literature.

The interaction of the carboxylic acid on the naphthalene ring is of great importance in determining its structure and vibrational properties. The naphthalene ring moiety is essentially coplanar with carboxylic acid group as evident from the dihedral angles [C8–C7–C6–O3 = 0.002º and C8–C7–C6–O1 = –179.995º]. It is observed that the influence of the substituent on the molecule play a vital role particularly in the C–C bond distance of the ring carbon atoms. As can be seen from Table 1, the calculated bond lengths around the carboxylic acid of C8–C9, C7–C8 and C21–C7 are 1.433, 1.405 and 1.427 Å, show slight deviation when compared with C19–C21, C10–C12 and C14–C16 of 1.367 1.379, and 1.379 Å.

4.2 Conformational analysis

Visualizing and describing the relationship between potential energy and molecular geometry is

Table 1 – Optimized geometrical parameters of 1H2NA calculated at the DFT/B3LYP level with 6–31G(d,p) basis set

Parameters	Exp.[6]	Monomer	Dimer		Exp.[6]	Monomer	Dimer
Bond lengths (Å)				Bond angles (º)			
C6–O1	1.321(2)	1.348	1.317	H2–O1–C6	113(2)	105.99	110.70
C6–O3	1.243(3)	1.237	1.258	H5–O4–C8	107(2)	106.76	106.84
O1–H2	0.94(5)	0.972	1.003	O1–C6–O3	121.1(2)	120.32	121.84
C6–C7	1.451(4)	1.459	1.459	O1–C6–C7	115.1(2)	115.10	116.15
C7–C8	1.390(2)	1.405	1.405	O3–C6–C7	123.8(2)	124.58	122.01
C8–O4	1.341(3)	1.337	1.339	C6–C7–C8	119.6(2)	118.24	119.60
O4–H5	0.87(4)	0.992	0.989	C6–C7–C21	120.7(2)	122.01	120.82
C8–C9	1.438(4)	1.433	1.433	C8–C7–C21	119.7(2)	119.75	119.57
C9–C18	1.410(4)	1.429	1.428	O4–C8–C7	123.6(2)	122.64	122.96
C18–C19	1.423(3)	1.428	1.428	O4–C8–C9	116.3(2)	117.32	116.96
C19–H20	0.930	1.086	1.086	C7–C8–C9	120.1(2)	120.04	120.08
C19–C21	1.346(5)	1.367	1.366	C8–C9–C10	121.2(2)	121.20	121.16
C21–H22	0.930	1.084	1.084	C8–C9–C18	118.5(2)	118.95	119.02
C21–C7	1.425(4)	1.427	1.428	C10–C9–C18	120.3(2)	119.86	119.82
C9–C10	1.408(3)	1.417	1.417	C9–C10–C12	119.5(2)	120.35	120.34
C10–H11	0.929	1.084	1.084	C10–C12–C14	120.7(3)	120.12	120.14
C10–C12	1.369(6)	1.379	1.379	C12–C14–C16	121.4(3)	120.48	120.48
C12–H13	0.930	1.086	1.086	C14–C16–C18	119.7(3)	120.93	120.91
C12–C14	1.387(6)	1.413	1.413	C9–C18–C16	118.5(2)	118.25	118.31
C14–H15	0.929	1.086	1.086	C9–C18–C19	120.0(2)	119.69	119.63
C14–C16	1.368(3)	1.379	1.379	C16–C18–C19	121.5(2)	122.06	122.07
C16–H17	0.930	1.087	1.087	C18–C19–C21	120.7(2)	120.51	120.50
C16–C18	1.418(5)	1.418	1.417	C7–C21–C19	121.0(2)	121.06	121.20
				Dihedral angles (º)			
C7–C8–O4–H5	1(2)	0.003	0.001	C10–C9–C8–C7	-179.5(2)	179.999	-179.996
O3–C6–O1–H2	2(2)	0.003	0.202	C18–C9–C8–C7	0.1(3)	0.000	-0.006
C7–C6–O1–H2	-178(2)	-179.999	-179.793	C12–C10–C9–C8	-179.6(2)	179.997	179.986
C9–C8–O4–H5	-179(2)	-179.995	179.995	C12–C10–C9–C18	0.8(4)	-0.004	-0.005
C8–C7–C6–O1	179.0(2)	-179.995	-179.954	C16–C18–C9–C8	179.9(2)	-179.998	-179.987
C21–C7–C6–O1	-1.3(3)	0.006	0.008	C16–C18–C9–C10	-0.5(3)	0.002	0.004
C8–C7–C6–O3	-1.0(4)	0.002	0.051	C19–C18–C9–C10	179.6(2)	179.999	-179.995
C21–C7–C6–O3	178.8(2)	-179.996	-179.979	C14–C12–C10–C9	-0.9(4)	0.004	0.002
O4–C8–C7–C6	0.2(3)	0.005	-0.045	C16–C14–C12–C10	0.8(5)	-0.004	0.003
C9–C8–C7–C6	-180.0(2)	-179.997	179.961	C18–C16–C14–C12	-0.5(4)	0.003	-0.004
O4–C8–C7–C21	-179.6(2)	-179.997	179.985	C9–C18–C16–C14	0.3(4)	-0.002	0.000
C9–C8–C7–C21	0.3(3)	0.001	-0.009	C19–C18–C16–C14	-179.7(3)	-179.999	179.999
C19–C21–C7–C6	179.5(2)	179.998	-179.954	C21–C19–C18–C9	-0.4(4)	0.002	-0.007
C19–C21–C7–C8	-0.7(3)	0.001	0.017	C21–C19–C18–C16	179.7(2)	179.999	179.993
C10–C9–C8–O4	0.4(3)	-0.003	0.010	C7–C21–C19–C18	0.8(4)	-0.003	-0.008
C18–C9–C8–O4	180.0(2)	179.998	-180.000				
Intermolecular H bond lengths				Intermolecular H bond angles			
H2··· O38 (H40···O3)			1.645(1.643)	O1–H2···O38			177.961
O3··· O39 (O1···O38)			2.646(2.648)	O39–H40···O3			177.915

called a potential energy surface (PES) that is an important to reveal all possible conformations of the title molecule. A detailed PES scan for O–H bond in the naphthalene ring has been performed at the DFT/B3LYP/6–31G (d,p) method to determine the most stable conformers of 1H2NA. For the modelling of the PES scan, the initial guess of N2HES was taken from the X-ray coordinates. According to X–ray study[6], dihedral angle of C7–C8–O4–H5 is 0.0º, whereas it has been calculated at 210.0º for the DFT/B3LYP method, leading to an expected bent conformation of the molecule. For conformational analysis of the studied molecule, starting from the optimized molecular structure given in Fig. 2, the C7–C8–O4–H5 dihedral angle was increased by 10° steps from 0° to 210°, while all of the other geometrical parameters have been simultaneously relaxed. PES scan for the selected dihedral angle is depicted in Fig. 2. For the C7–C8–O4–H5 rotation, the minimum energy was obtained at 0.0°. The barrier of this rotation for 0.0° is –649.718 hartree, clearly showing that hydroxyl group in the naphthalene ring

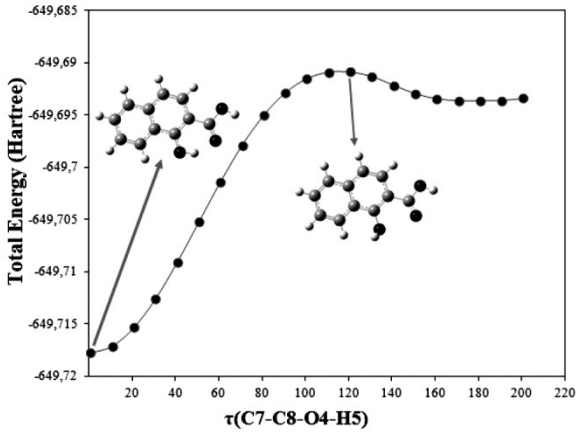

Fig. 2 – One-dimensional potential energy surface (PES) scan of l-hydroxy-2-naphthoic acid acid using DFT/B3LYP level with 6–31G(d,p) basis set.

is to form the intramolecular hydrogen bonding at this position. For the C7–C8–O4–H5 rotation, one maximum energy position was obtained at 120° in the potential energy curve of energy −649.691 hatree, clearly showing that the hydroxyl group has no chance of forming the intramolecular hydrogen bonding in that angle.

4.3 FMO and ultraviolet–visible (UV–Vis) spectral analysis

The most important orbitals in a molecule are the frontier molecule orbitals (FMOs), called the highest occupied molecular orbital (HOMO) and the lowest unoccupied molecular orbital (LUMO). These orbitals play a significant role in electronic, electric and optical properties as well as in the quantum chemistry and UV–Vis spectra[23]. The energy of LUMO is directly related to the electron affinity (*A*) and characterizes the susceptibility of the molecule towards attack by nucleophiles. The energy of the HOMO is directly related to the ionization potential (*I*) and characterizes the susceptibility of the molecules towards attack by electrophiles[24]. The energy difference between the LUMO and HOMO energies which is called as energy gap reflects the chemical reactivity and kinetic stability of the molecule. Meanwhile, a molecule with a small frontier orbital gap (higher is the flow of electrons to the lesser energy state) is more polarizable and is generally associated with a high chemical reactivity, low kinetic stability and is also termed as soft molecule[22,25]. The 3D plots of the HOMO and LUMO for 1H2NA using the DFT/B3LYP/6–31G (d,p) calculation for gas phase are shown in Fig. 3(a and b). The positive phase is represented by the red color and

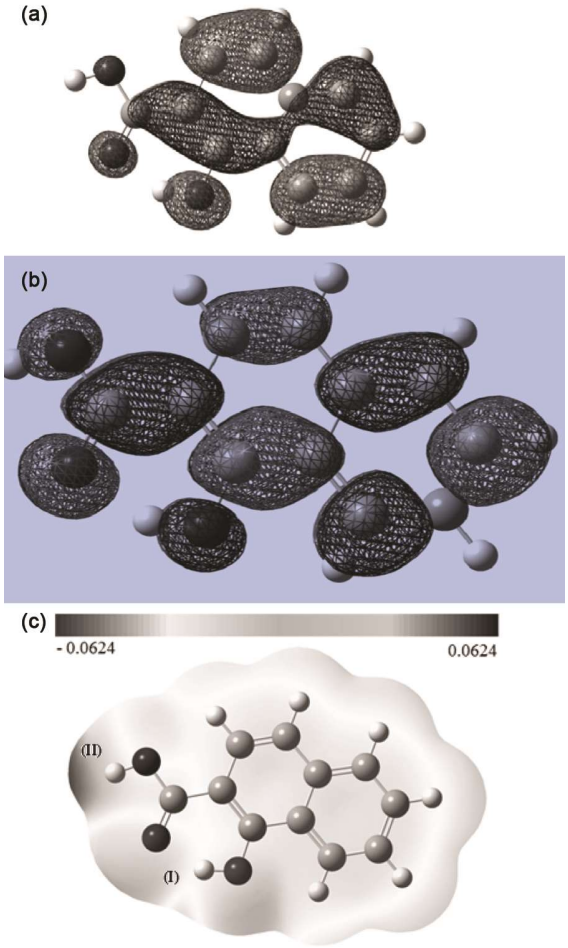

Fig. 3 – The 3-D orbital pictures of (a) the HOMO, (b) the LUMO and (c) the molecular electrostatic potential (MEP) by the DFT/B3LYP/6–31G (d,p) level for 1H2NA.

the negative one is by the green color. The HOMO is localized mainly on all atoms and expect of OH group, but LUMO is characterized by a charge distribution on all molecule expect of hydrogen atoms in OH group and naphthalene ring. The total energy, HOMO and LUMO energies, and the $\Delta E_{\text{LUMO–HOMO}}$ energy gap calculations in solvent and gas phase were performed by using the time dependent density functional theory (TD–DFT) and the values are presented in Table 2. The energy values of LUMO are calculated as –1.427 eV (in gas phase) and –1.528 eV (in ethanol), the HOMO are calculated as –5.765 eV (in gas phase) and –5.861 eV (in ethanol) and the energy gap values are found to be 4.338 eV (in gas phase) and 4.333 eV (in ethanol) obtained at TD–DFT/B3LYP method with 6–31G (d,p) basis set. Moreover lower in the energy gap of HOMO – LUMO explains the eventual charge transfer

Table 2 – Total energy (in a.u.), E_{HOMO}, E_{LUMO}, $\Delta E_{LUMO–HOMO}$, ionization potential I, electron affinity A, global hardness η, chemical potential Pi, electrophilicity index ω, (all in eV), and global softness σ, (in eV^{-1}) values of 1H2NA using the TD–DFT/B3LYP/6–31G(d,p) method.

	Gas	Ethanol
Total energy	–649.427	–649.435
E_{HOMO}	–5.765	–5.861
E_{LUMO}	–1.427	–1.528
$\Delta E_{LUMO–HOMO}$	4.338	4.333
I	5.765	5.861
A	1.427	1.528
η	2.169	2.167
σ	0.461	0.462
Pi	–3.596	–3.695
ω	2.981	3.150

interaction within the molecule and the frontier orbital energy gap of the studied molecule. Furthermore, in going from the gas phase to the solvent phase, the decreasing value of the energy gap and molecule becomes more reactive.

Gauss-Sum 3.0 program[26] was used to prepare the density of states (DOS) spectra in Fig. 4. In general, positive value of DOS indicates a bonding interaction, negative value means that there is an anti-bonding interaction and zero value indicates non-bonding interactions[27]. DOS plot shows an easy understanding of the molecular orbitals character in a certain energy range and energy gap of a molecule.

The UV–Visible spectral analysis was carried out in order to understand the nature of electronic transitions of 1H2NA. The TD-SCF calculation has been used to find out the absorption wavelengths (λ), excitation energies (E) and oscillator strengths (f) for 1H2NA in gas phase and ethanol solution. The oscillator strengths, absorption wavelengths, and excitation energies were calculated by using the TD–DFT/6–31G (d,p) method with solvent and gas phase and were given in Table 3. The simulated and experimental absorption spectra of the studied molecule with solvent and gas phase were shown in Fig. 5. The calculated absorption wavelengths (λ) in ethanol solvent and gas phase were found to be 239.45, 321.13, and 233.82, 318.16 nm with excitation energies 5.1778, 3.8609, and 5.3025, 3.8970 at the TD–DFT/B3LYP/6–31G (d,p) method, respectively. The TD–DFT calculations demonstrate that the electronic absorption at the highest wavelength chiefly formed by two electronic transition modes H–1 →L(60.45%) and H–2 → L(73.07%) is found to be 239.45 nm (in ethanol solvent) and 233.82 nm (in gas phase) with minor

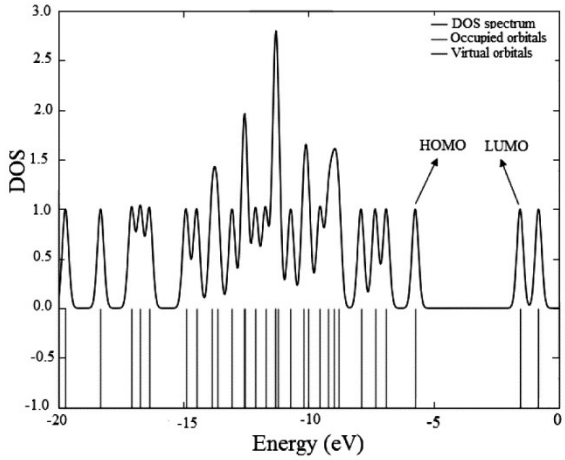

Fig. 4 – Density of states (DOS) diagrams for l-hydroxy-2-naphthoic acid.

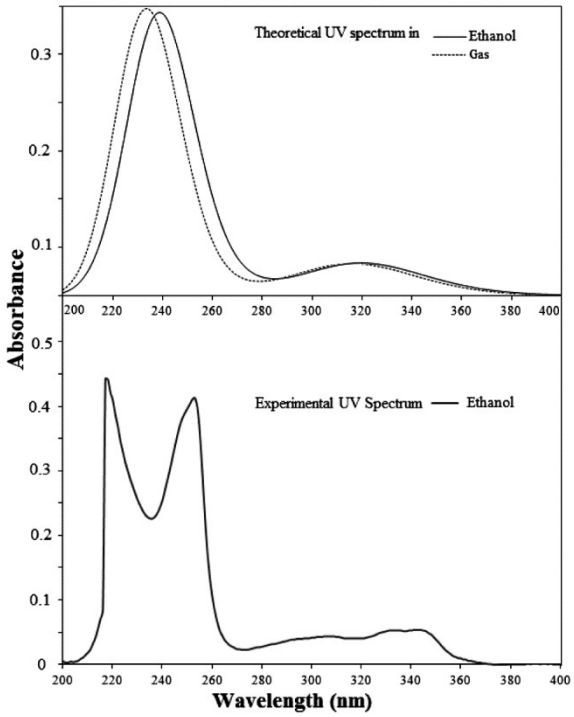

Fig. 5 – The experimental and simulated UV–Vis absorption spectra of 1H2NA at DFT/B3LYP/6–31G (d,p) level.

difference of percent. In 1H2NA, the experimental absorption bands are viewed at 217.00, 253.00 and 342.00 nm with excitation energies 5.7713, 4.9005 and 3.6252 eV, respectively.

4.4 Molecular electrostatic potential (MEP) analysis

The molecular electrostatic potential (MEP) is useful quantities that are applied to illustrate the charge distributions of molecules and to visualize variably charged regions of molecules. MEP is a

Table 3 – The experimental and theoretical electronic absorption spectra of l-hydroxy-2-naphthoic acid using the TD–DFT/B3LYP/6–31G(d,p) method in solvent and gas phase.

Experimental			Calculated				Major contributions
	λ (nm)	E (eV)		λ (nm)	f (a.u)	E (eV)	
Ethanol	217.00	5.7135	Ethanol	-	-	-	-
	253.00	4.9005		239.45	0.8901	5.1778	H–1→L(60.45%), H→L+1(23.78%)
	342.00	3.6252		321.13	0.1057	3.8609	H→L(91.98%)
	-	-	Gas	233.82	0.1540	5.3025	H–2→L(73.07%)
	-	-		318.16	0.0786	3.8970	H→L(90.40%)

helpful tool for understanding sites of electrophilic and nucleophilic reactions as well as hydrogen bonding interactions on organic molecules[28]. The strongest attraction is represented by the positive (blue color) region, whereas the strongest repulsion is represented by the negative (red color) region. The negative (red, orange, and yellow) regions of MEP are related to electrophilic reactivity and the positive (blue color) ones belong to nucleophilic reactivity. To predict reactive sites of electrophilic and nucleophilic attack for the title molecule, Fig. 3(c) shows the 3D plot of molecular electrostatic potential surface for 1H2NA molecule that was calculated at the DFT/B3LYP/6–31G (d,p) level. As can be seen in Fig. 3(c), the MEP map of the studied molecule clearly suggests that the maximum positive potential region (II) localized on the hydrogen atom in the carboxylic group has a value of +0.0624 a.u., indicating the possible sites for nucleophilic attack. The MEP map Fig. 3(c) shows that the negative potential sites (I) correspond to the electronegative the oxygen atom for carboxylic acid and OH atoms in the naphthalene ring. These sites provide information about the region in which the compound can have intermolecular interactions. From these results, we can conclude that the H atom in the carboxylic group is the locations of the strongest attraction and O atoms indicate the strongest repulsion.

4.5 Global reactivity descriptors

The understanding of chemical reactivity and stability of the molecular systems has been effectively handled by the conceptual density functional theory (DFT)[29]. Global hardness (η), global softness (σ), chemical potential (Pi) and electrophilicity index (ω) are global reactivity descriptors, highly successful in predicting global chemical reactivity trends. Various reactivity descriptors as global hardness (η), global softness (σ), chemical potential (Pi), and electrophilicity index (ω) were calculated using the time dependent density functional theory (TD–DFT) level with the 6–31G (d,p) basis set in ethanol solvent and gas phase and are presented in Table 2. The chemical stability and reactivity of the chemical system are completely based on its hardness and properties, which is resist to intramolecular charge transfer. The lower value of $\Delta E_{\text{LUMO–HOMO}}$ represent, the molecule will be soft, more reactivity and weak stability. The values of η and σ of the title molecule are 2.169 eV (0.461 eV^{-1}) and 2.167 eV (0.462 eV^{-1}) in gas phase and ethanol solvent, respectively. As can be seen from Table 2, it may be observed that the global hardness of the studied molecule de creases when solvent was taken into account. Obtained small η value means that the charge transfer occurs in the studied compound. The electrophilicity index ω measures the susceptibility of chemical species to accept electrons. Thus, low values of ω suggest a good nucleophile while higher values indicate the presence of a good electrophile. Moreover, the values of ω are bigger in the ethanol solvent in comparison to the gas phase, this fact would suggest that electrophile behavior increases on the studied molecule in the presence of solvents.

4.6 Atomic net charges

The atomic charges have an important role in the application of quantum chemical calculations of molecular system because of the atomic charges affect dipole moment, polarizability, electronic structure, vibrational spectra and more properties for a molecular system[30]. The atomic charges of 1H2NA by Mulliken population and natural bond orbital (NBO) analysis using the DFT/B3LYP level with the 6–31G (d,p) basis set in gas phase were calculated and obtained results are presented in Fig. 6 and Table 4.

The C6 and C8 atoms connected with highly electro negative oxygen atoms making that particular carbon more electron deficient. So that it gets more positive and acidic. C10, C12, C14, C16, C18, C19 and C21 carbon atoms, except that C6 and C8 in the naphthalene ring and carboxylic group have

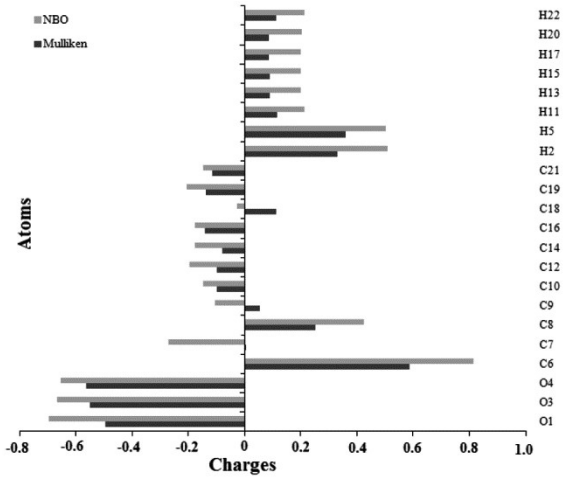

Fig. 6 – Histogram of Mulliken and natural bond orbital atomic charges for 1H2NA at the DFT/B3LYP/6–31G (d,p) level.

Table 4 – Atomic charges distribution of the title compound calculated by the Mulliken and natural bond orbital (NBO) methods using the B3LYP/6–31G(d,p) level in gas phase.

Atoms	Mulliken	NBO
O1	-0.497	-0.697
O3	-0.550	-0.668
O4	-0.564	-0.655
C6	0.588	0.813
C7	0.004	-0.272
C8	0.253	0.425
C9	0.055	-0.104
C10	-0.098	-0.147
C12	-0.099	-0.197
C14	-0.080	-0.178
C16	-0.141	-0.177
C18	-0.111	-0.027
C19	-0.137	-0.206
C21	-0.115	-0.148
H2	0.330	0.510
H5	0.359	0.501
H11	0.115	0.212
H13	0.091	0.201
H15	0.091	0.199
H17	0.088	0.200
H20	0.085	0.203
H22	0.111	0.213

negative charges since these atoms are bounded to electronegative O atom. The presence of two O atoms in naphthalene ring and carboxylic group, because of more electro negativity, makes all these carbon atoms C10, C12, C14, C16, C18, C19 and C21 more negative. As can be seen in Fig. 6, the negative charges mainly located on O1, O3 and O4 atoms will interact with the positive part of the receptor. On the contrary, C6 and C8 are the most positively charged part, which can interact with the negatively charged part of the receptor easily.

All hydrogen atoms have positive charges varied in the range of 0.085–0.359 and 0.199–0.510 obtained by Mulliken and NBO analysis for the DFT/B3LYP level with the 6–31G (d,p) basis set, respectively. The presence of two N atoms in pyridazine ring and two O atoms in carboxylic group, because of more electro negativity, makes these carbon atoms C1, C4, and C5 more negative. All the H atoms in pyridazine ring as well as in carboxylic group are positive as they lose their electrons to the nearby carbon atoms. When magnitudes of the charge of each atom predicted by the two methods are compared, the magnitude predicted by B3LYP is more for each atom than that predicted by HF method even though the basis set is same.

4.7 Non-linear optical (NLO) properties

Density functional theory has been used as an effective method to investigate the organic nonlinear optical (NLO) materials. In the current study, the NLO effect is considered most important because it provides key functions of optical modulation, optical switching, optical logic and optical memory for the emerging technologies in the areas of telecommunications, optical interconnections and signal processing[31]. In order to investigate the effects of the DFT/B3LYP method on the NLO properties of the studied compound, the dipole moments (μ), the polarizabilities (α), the anisotropy of the polarizabilities ($\langle\Delta\alpha\rangle$) and the mean first-order hyperpolarizabilities (β) of 1H2NA were calculated using the finite-field approach and are presented in Table 5.

As can be seen from Table 5, the calculated value of the dipole moment is found to be 2.2744 D for the DFT/B3LYP level, almost independent of the basis set and the stronger dipole moment in the case of the studied compound is primarily attributed to an overall imbalance in the charge from one side of a molecule to the other side. The highest value of the dipole moment is observed for component μ_y. In this direction, this value is equal to 2.2248 D and μ_z is the smallest one as 0.1600 D. Here, the high dipole moment value for the monomeric species of 2.2248 Debye suggests the formation of intermolecular H-bonds in the dimer while the about zero value (0.0180 D) of dipole moment confirms the centro symmetric structure of the dimer. As shown in Table 5, the calculated polarizabilities are dominated by the

Table 5 – Dipole moment μ (D), mean polarizabity $<\alpha>$ (in a.u. and esu), the anisotropic of the polarizability $<\Delta\alpha>$ (in a.u.) and the mean first-order hyperpolarizability β (in a.u. and esu) values obtained using B3LYP/6–31G(d,p) method for l-hydroxy-2-naphthoic acid.

Parameters	B3LYP	Parameters	B3LYP	Parameters	B3LYP
μ_x	0.4446	α_{xx}	187.5833	β_{xxx}	–631.5450
μ_y	2.2248	α_{xy}	–1.3079	β_{xxy}	8.4507
μ_z	0.1600	α_{yy}	40.6274	β_{xyy}	4.9880
$\mu_{monomer}$	2.2744	α_{xz}	11.6044	β_{yyy}	–0.8398
μ_{dimer}	0.0180	α_{yz}	2.7672	β_{xxz}	–37.6715
		α_{zz}	122.4464	β_{xyz}	5.9896
		$<\alpha>$ *(a.u.)*	116.8857	β_{yyz}	–3.5214
		$<\alpha>x10^{-24}$ *(esu)*	17.3225	β_{xzz}	143.9380
		$<\Delta\alpha>$ *(a.u.)*	129.2235	β_{yzz}	–1.7767
		$<\Delta\alpha>$ $x10^{-24}$ *(esu)*	19.1509	β_{zzz}	–35.4357
				β *(a.u)*	488.6993
				β_{tot} $x\ 10^{-30}$ *(esu)*	4.2220
				β_{tot}/β_{urea}	22

diagonal components. The calculated polarizability and the anisotropy of the polarizability values are equal to 17.3225×10^{-24} and 19.1509×10^{-24} esu for the DFT/B3LYP/6–31G (d,p) method, respectively. The simulations exclusively based on DFT method are capable of providing better results in principle. The magnitude of the mean first-order hyperpolarizability (β) is one of the key factors in NLO systems. In this study, the mean first-order hyperpolarizability (β) was calculated at 4.2220×10^{-30} esu using the DFT/B3LYP level. Urea is one of the prototypical molecules used for studying the NLO properties of the molecular systems. Therefore, it is frequently used as a threshold value for comparative purposes. The value of β and $\langle\alpha\rangle$ of 1H2NA are 4.2220×10^{-30} and 17.3225×10^{-24} esu for the DFT method with the same basis set. The β and $\langle\alpha\rangle$ values obtained from the DFT/B3LYP level are approximately 22 and 5 times greater than the magnitude of urea (for urea β and $\langle\alpha\rangle$ values are found to be 0.1947×10^{-30} and 3.8312×10^{-24} esu), respectively. The mean first-order hyperpolarizability component is very useful and it is clearly indicates the direction of charge delocalization. Therefore, the largest β_{xxx} value indicates charge delocalization along with the 'xxx' direction. The β value calculated by the DFT/B3LYP method shows that the title compound is an attractive molecule for future studies of NLO properties. Based on NLO properties of (common values) urea; the mean first-order hyperpolarizability and polarizability values of the studied molecule are bigger than those of urea.

4.8 Natural bond orbital (NBO) analysis

The natural bond orbital (NBO) analysis provides an efficient method for studying intra and inter-molecular bonding and interaction among bonds and also provides a convenient basis for investigating charge transfer or conjugative interaction in molecular systems[32]. The NBO calculation used to understand various second order interactions between the filled orbitals of one subsystem and vacant orbitals of another subsystem, which is a measure of the inter-molecular delocalization or hyper conjugation. The interaction result is a loss of occupancy from the localized NBO of the idealized Lewis structure into an empty non-Lewis orbital. For each donor NBO (i) and acceptor NBO (j), the stabilization energy E (2) associated with electron delocalization between donor and acceptor is estimated as:

$$E(2) = \Delta E_{ij} = q_i \frac{F^2_{(i,j)}}{\varepsilon_j - \varepsilon_i} \quad \ldots (8)$$

Where, q_i is the donor-orbital occupancy, ε_j and ε_i are diagonal elements orbital energies and $F_{(i,j)}$ is the Fock matrix element between the natural bonding orbitals. The larger the E(2) value, the more intensive is the interaction between electron donors and electron acceptors, i.e., the more donating tendency from electron donors to electron acceptors and the greater the extent of conjugation of the whole system.

The natural bond orbitals (NBO) calculations for 1H2NA were performed using NBO 3.1 program[33] as implemented in the Gaussian 09 package at the DFT/B3LYP/6–31G (d,p) method. The NBO analysis has been performed to elucidate the intramolecular interaction, rehybridization and delocalization of electron density within the molecule, which are presented in Table S1. In order to investigate the intramolecular hydrogen bonding, intermolecular hydrogen bonding, intermolecular charge transfer (ICT), the stabilization energies due to LP(O) → σ*(O–H), NBO analysis of the title compound were computed by using second-order perturbation theory. The corresponding results of second-order perturbation theory analysis of Fock matrix at the DFT/B3LYP level with 6–31G (d,p) basis set of title compound are given in Table S2. In this Table S2 summarized the stabilization energies of donor–

acceptor interactions with more than 1.5 kcal/mol determined by second order perturbation analysis of Fock matrix.

The higher the *E* (2) value, the stronger is the interaction between electron donors and electron acceptors, and reveals a more donating tendency from electron donors to electron acceptors and a greater degree of conjugation of the whole system. The second order perturbation theory analysis of Fock matrix in NBO basis of 1H2NA indicates a remarkable stabilization (32.63 kcal/mol) due to the orbital overlap between anti-bonding π(C7–C8) and anti-bonding π*(O3–C6). The system is also stabilized due to the interactions between the π type orbital containing lone pairs of electron of O1(LP2) and O3(LP2) with anti-bonding π*(O3–C6) and π*(O1–C6) orbitals, respectively resulting in the stabilization of carboxylic acid structure due to the resonance delocalization. The magnitude of charge delocalization amounts to stabilization of ca. 52 and 29 kcal/mol in the two cases.

In the molecule, a strong intramolecular hyperconjugative interaction of π-electrons with the greater energy contributions from C7–C8 → C19–C21 (18.61 kcal/mol for the DFT/B3LYP level), C10–C12 → C14–C16 (20.35 kcal/mol for the DFT/B3LYP level), C14–C16 → C10–C12 (17.96 kcal/mol for the DFT/B3LYP level), and C19–C21 → C7–C8 (12.91 kcal/mol for the DFT/B3LYP level) for the naphthalene ring of the studied molecule.

In Table S2, BD(1) O1–H2 orbital with 1.98774 electrons has 76.05% O1 character in a $sp^{3.17}$ hybrid and has 23.95% H2 character in a sp hybrid. The $sp^{3.17}$ hybrid on O1 has 75.95% p-character and the sp hybrid on H2 has 0.22% p-character in the DFT/B3LYP/6–31G (d,p) method.

4.9 Vibrational analysis

The vibrational spectra of 1H2NA have not been described in detail in any literature. Therefore, the observed and simulated FT–IR and FT–Raman spectra of the studied molecule were shown in Fig. 7 and 8, respectively. Experimental wave numbers with the calculated wave numbers using the DFT/B3LYP level with their potential energy distributions (PEDs) for monomer and dimer conformers of studied molecule are tabulated in Table 6. The scale factor is used to obtain the best agreement results between the calculated and experimental frequencies. The vibrational frequencies for the title compound are calculated with this method and then wave numbers are scaled with 0.9614 in the DFT/B3LYP level[34].

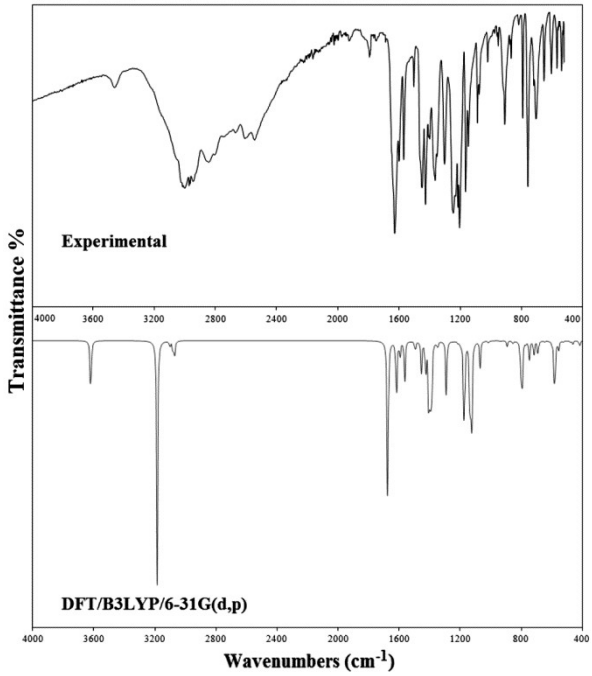

Fig. 7 – Comparison of the observed and simulated FT–IR spectra computed at the DFT/B3LYP level with 6–31G (d,p) basis set of 1H2NA.

4.9.1 COOH vibrations

The carboxylic acid O–H stretching band is weak in the FT–Raman spectrum, so FT–IR data is generally used. The O–H stretching band[35] is characterized by very broad band appearing near about 3400–3600 cm^{-1}. For salicylic acid[36], the O–H vibration is observed to 3238 cm^{-1} in FT–IR spectra. Karabacak *et al*.[37] calculated these O–H stretching bands calculated at 3609 and 3339 cm^{-1} (5-fluoro-salicylic acid) and 3608 and 3330 cm^{-1} (5-chloro-salicylic acid) which modes are (ν1, ν2) of O11 –H12, O14 –H15 units, respectively. The carboxylic acid O–H stretching band observed in 3454 cm^{-1} in the FT–IR spectrum and calculated at 3622 cm^{-1} using the DFT/B3LYP/6–31G (d,p) method for naphthoic acid[19]. In the present study, this band at 3460 cm^{-1} in FT–IR spectrum is assigned to the carboxylic acid O–H stretching vibration and its corresponding value is calculated at 3620 cm^{-1} for monomeric structure using the DFT/B3LYP level. It is true from PED value contributing to 100%, suggested pure stretching mode as it is evident from PED column (mode no 1). In the present study, the O–H stretching vibration in the naphthalene ring is calculated at 3184 and 3253, 3251 cm^{-1} which have the PED value 99% for monomeric and dimeric structures using the DFT/B3LYP level, respectively. The O–H stretching

Table 6 – Comparison of the observed (FT–IR and FT–Raman) and calculated vibrational wave numbers with potential energy distribution (PED) using the DFT/B3LYP/6–31G(d,p) method of monomer and dimer conformer of 1H2NA.

		Experimental		Monomeric		Dimeric	
ν	Assignments (%PED[a])	FT–IR	FT–Raman	unscaled	scaled	unscale	scaled
1	ν(OH) (100)	3460	-	3765	3620	3168, 3073	3045, 2954
2	ν(OH) (99)	3062	3068	3312	3184	3384, 3382	3253, 3251
3	ν(CH) (84)	-	3049	3227	3102	3230, 3230	3105, 3105
4	ν(CH) (87)	3016	3014	3226	3101	3228, 3228	3103, 3103
5	ν_{as}(CH) (93)	-	-	3204	3080	3205, 3205	3081, 3081
6	ν_{as}(CH) (92)	-	-	3193	3070	3195, 3195	3072, 3072
7	ν_{as}(CH) (92)	2972	-	3179	3056	3181, 3181	3058, 3058
8	ν(C=O)(66)	1632	1633	1742	1675	1702, 1702	1636, 1636
9	ν(CC)(47)	-	-	1683	1618	1684, 1681	1619, 1616
10	ν(CC)(49)	1602	1606	1658	1594	1658, 1653	1594, 1589
11	ν(CC)(30), σ(HOC)(12), β(CCC)(10)	1572	1576	1626	1563	1625, 1622	1562, 1559
12	δ(HCC)(14)	1506	1506	1555	1495	1555, 1553	1495, 1493
13	δ(HCC)(27), σ(HOC)(18)	1452	1468	1513	1455	1513, 1507	1455, 1449
14	σ(HOC)(10), ν(CC)(10)	1429	1444	1483	1426	1476, 1470	1419, 1413
15	ν(OC)(11), σ(HOC)(15), σ(HCC)(18)	1402	1417	1463	1407	1461, 1460	1405, 1404
16	ν(CC)(11)	-	1383	1453	1397	1447, 1443	1391,1387
17	δ(HCC)(10), ν(OC)(11)	1365	-	1443	1387	1409, 1406	1356, 1352
18	ν(CC)(46)	1354	1317	1403	1349	1406, 1383	1352, 1330
19	ν(CC)(10), σ(HOC)(13)	1306	1290	1342	1290	1326, 1319	1275, 1268
20	δ(HCC)(32), ν(CC)(10)	1248	1259	1301	1251	1294, 1292	1244, 1242
21	σ(HCC)(23), ν(OC)(16)	1217	1213	1262	1213	1258, 1257	1209, 1209
22	ν(CC)(24), δ(HCC)(27)	1207	-	1244	1196	1243, 1243	1195, 1195
23	ν(CC)(24), σ(HOC)(33)	1169	1167	1221	1174	1208, 1205	1161, 1159
24	σ(HCC)(68)	1149	1151	1184	1138	1184, 1184	1138, 1138
25	σ(HCC)(47), ν(CC)(13)	1135	1117	1181	1135	1179, 1179	1133, 1133
26	ν(OC)(26), σ(HOC)(15)	1090	1090	1171	1126	-	-
27	β(CCC)(25)	1078	1074	1112	1069	1116, 1116	1073, 1073
28	ν(CC)(53)	1024	1024	1055	1014	1055, 1055	1014, 1014
29	γ(HCCC)(82), γ(CCCC)(12)	978	974	1001	962	1001, 1001	962, 962
30	γ(HCCC)(85)	955	947	975	937	977, 977	939, 939
31	γ(HCCC)(69)	-	928	967	930	969, 969	932, 932
32	ν(OC)(13), ν(CC)(12), β(CCC)(16)	912	912	929	893	939, 937	903, 901
33	γ(HCCC)(76)	878	877	891	857	891, 891	857, 857
34	β(CCC)(58)	822	827	886	852	889, 888	855, 854
35	γ(OCOC)(12), γ(HOCC)(58)	795	796	836	804	831, 831	799, 799
36	γ(HOCC)(26), γ(HCCC)(39)	-	785	827	795	806, 805	775, 774
37	γ(CCCC)(22), γ(OCCC)(16), γ(HCCC)(15)	760	-	801	770	799, 799	768, 768
38	γ(HCCC)(46), γ(OCOC)(25)	721	723	778	748	776, 775	746, 745
39	γ(OCOC)(32), γ(HCCC)(19)	708	-	747	718	743, 742	714, 713
40	β(CCC)(29), β(OCO)(18)	656	681	718	690	738, 735	710, 707
41	γ(OCOC)(10), γ(OCCC)(32)	-	642	673	647	669, 667	643, 641
42	ν(CC)(18), β(CCC)(15), β(OCC)(12)	608	615	620	596	632, 630	608, 606
43	γ(HOCC)(56)	-	596	605	582	-	-

(*Contd.*)

Table 6 – Comparison of the observed (FT–IR and FT–Raman) and calculated vibrational wave numbers with potential energy distribution (PED) using the DFT/B3LYP/6–31G(d,p) method of monomer and dimer conformer of 1H2NA.

		Experimental		Monomeric		Dimeric	
		FT–IR	FT–Raman	unscaled	scaled	unscale	scaled
44	β(OCO)(46)	571	569	602	579	616, 615	592, 591
45	γ(HOCC)(28), γ(CCCC)(24)	540	542	578	556	587, 587	564, 564
46	β(CCC)(17), β(OCC)(21)	525	491	545	523	556, 551	535, 530
47	β(CCC)(47), ν(CC)(10)	-	476	497	478	501, 499	482, 480
48	γ(CCCC)(53)	-	461	481	462	489, 488	470, 469
49	ν(CC)(11), β(OCC)(57)	-	426	436	419	474, 442	456, 425
50	γ(CCCC)(47)	-	-	433	416	433, 433	416, 416

Abbreviations; ν, stretching; β, in-plane bending; σ, scissoring; δ, rocking; γ, out-of-plane bending; τ, torsion; ω, wagging; s, simetric; as, antisimetric.

[a] Potential Energy Distribution (PED) less then 10% are not shown.

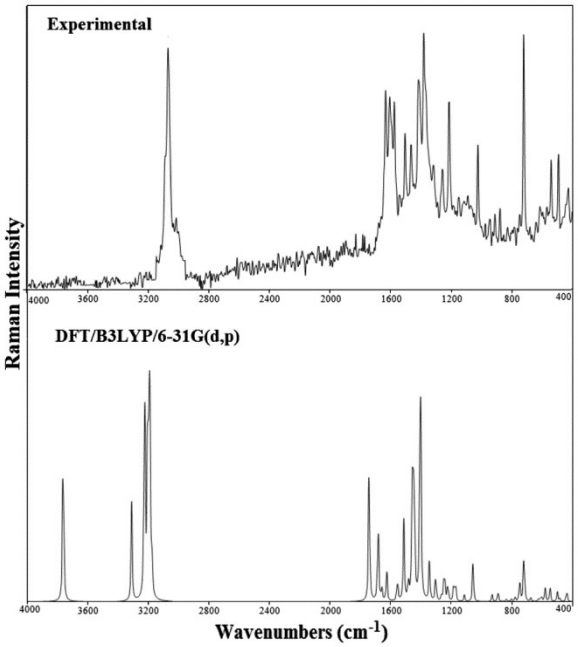

Fig. 8 – Comparison of the observed and simulated FT–Raman spectra computed at the DFT/B3LYP level with 6–31G(d,p) basis set of 1H2NA.

vibration in the naphthalene ring is observed at 3062 cm^{-1} in the FT–IR spectrum and at 3068 cm^{-1} in the FT–Raman spectrum.

The carboxylic acid O–H in–plane bending and out–of–plane vibrations[38] usually appear in the range of 1440–1260 cm^{-1} and 720–600 cm^{-1}, respectively. The carboxylic acid O–H in–plane bending vibration is observed at 1306, 1169 and 1090 cm^{-1} in the FT–IR and at 1290, 1167, and 1090 cm^{-1} in the FT–Raman spectra. The carboxylic acid O–H in–plane bending vibration is calculated at 1290, 1174, and 1126 cm^{-1} for the DFT/B3LYP method. The bands observed at 1572, 1452 and 1402 cm^{-1} in the FT–IR spectrum and 1576, 1468 and 1417 cm^{-1} in the FT–Raman spectrum are assigned as O–H in–plane bending vibration in the naphthalene ring. These bands of 1H2NA are calculated at 1563, 1455 and 1407 cm^{-1} for the DFT/B3LYP method.

The observed bands at 795 cm^{-1} in FT–IR and at 796 and 596 cm^{-1} in FT–Raman spectra (mode no 35 and 43) are assigned as the O–H out–of–plane vibration in the naphthalene ring and carboxylic group, respectively. The O–H out–of–plane bending the naphthalene ring and carboxylic group of 1H2NA are calculated at 804 and 582 cm^{-1}. The PED values corresponding to this vibration are 58% and 56% for the DFT/B3LYP method, respectively. In dimer conformations, the O–H in–plane bending and out–of–plane bending vibrations values are generally increasing, because of the hydrogen bonding effect through the carboxyl groups (Table 6).

The C=O stretch of carboxylic acids[39] is identical to the C=O stretch in ketones, which is expected in the region 1740–1660cm^{-1}. The double bond between the carbon–oxygen atoms is formed by π-π bonding between carbon and oxygen. Because these atoms have different electro negativities, the bonding electrons are not equally distributed between the two atoms. The recorded band at 1632 cm^{-1} of 1H2NA in the FT–IR spectrum is assigned to C6=O3 stretching mode, which show very good agreement with the experimental FT–IR spectra in Zhang *et al.*[6]. The calculated frequency for the C6=O3 vibration was obtained at 1675 cm^{-1} which has the PED value 66% for DFT/B3LYP method (mode no. 8). Demir *et al.*[40] calculated the carbonyl (C=O) group stretching vibration at 1670 cm^{-1} using the B3LYP/6–31G (d) method. Krishnakumar *et al.*[41] reported the carbonyl (C=O) group stretching vibration of 6-bromo-2-

naphthoic acid as 1674 cm^{-1} with the B3LYP/6-311+G** level. However, the C=O stretching mode of dimer conformation was both calculated at 1636 cm^{-1} which is in very good agreement with experimental data because of the hydrogen-bonding effect the carboxyl groups. As can be seen in Table 6, the C=O stretching bond of the carboxylic acid dimer is observed near 1636 cm^{-1}, while the free acid band is observed at higher wave numbers (1675 cm^{-1}).

The C–O stretching vibration is normally observed at 1320–1210 cm^{-1} due to C–O stretching vibrations[42]. The C–O stretching vibrations observed at 1365, 1217 and 1090 cm^{-1} in the FT–IR spectrum and at 1213 and 1090 cm^{-1} in the FT–Raman spectrum calculated at 1387, 1213 and 1126 cm^{-1} which have the PED value 11%, 16%, and 26% using the DFT/B3LYP level.

4.9.2 C–H vibrations

The hetero aromatic organic compounds and their derivatives commonly exhibit multiple weak bands in the region 3100–3000 cm^{-1} which is the characteristic region for the ready identification of C–H stretching vibrations and these vibrations are not found to be affected due to the nature and position of the substituent[43,44]. In the present work, the vibrations ($v3$–$v7$) in Table 6 are assigned to C–H stretching modes. The $v3$, $v4$ and $v5$–$v7$ modes are symmetric and anti-symmetric C–H stretching vibrations, respectively. The theoretical vibrations assigned to C–H stretching obtained in the range of 3102–3056 cm^{-1} by the DFT/B3LYP method are show excellent agreement with the experimental values at 3016 and 2972 cm^{-1} in the FT–IR spectrum (3014 and 3049 cm^{-1} in the FT–Raman spectrum). As indicated by PED, these (symmetric and asymmetric) modes involve exact contribution of >84% suggesting that they are pure stretching modes.

In the aromatic compounds, the C–H in–plane and out–of–plane bending vibrations[38,45] generally lie in the region 1500–1100 and 1000–700 cm^{-1}, respectively. The FT–IR band at 1149 cm^{-1} and the FT–Raman band at 1151 cm^{-1} are assigned to C–H in–plane bending vibration of 1H2NA. The calculated frequency for the C–H in–plane bending vibration was obtained at 1138 cm^{-1} which has the PED value 68% for DFT/B3LYP method (mode no 24). The band indentified at 955 and 947 cm^{-1} in the FT–IR and FT–Raman spectra, respectively, has been designated to C–H out–of–plane bending bending mode. This bending vibration was computed at 937 cm^{-1} which has the PED value 85% by the DFT/B3LYP level.

4.9.3 C–C vibrations

Naphthalene ring stretching vibrations are expected in the region 1620–1390 cm^{-1}. Naphthalene ring vibrations are found to make a major contribution in the FT–IR and FT–Raman spectra[46,47]. The FT–IR bands at 1632, 1602, 1572, 1429, 1354, 1306, 1248, 1207, and 1169 cm^{-1} and the FT–Raman band at 1633, 1606, 1576, 1444, 1383, 1317, 1290, 1259, and 1167 cm^{-1} are assigned to C–C stretching vibrations of 1H2NA. In the present work, the theoretically predicated wave numbers at 1618, 1594, 1563, 1426, 1397, 1349, 1290, 1251, 1196, and 1174 cm^{-1} for the DFT/B3LYP method (mode no 9, 10, 11, 14, 16, 18, 19, 20, 22, and 23) are assigned as C–C stretching vibrations with PEDs contributions of 47, 49, 30, 10, 11, 46, 10, 10, 24, and 24%, respectively.

The bands observed at 1572, 1078, 912, 822, 656, 608, and 525 cm^{-1} in FT–IR spectrum and 1576, 1074, 912, 827, 681, 615, 491, and 476 cm^{-1} in FT–Raman spectrum are assigned to C–C–C in–plane bending vibration show good agreement with theoretically computed wave numbers at 1563, 1069, 893, 852, 690, 596, 523, and 478 cm^{-1} by BL3YP/6–31G (d,p) method (mode no 11, 27, 32, 34, 40, 42, 46, and 47) are assigned to C–C–C in–plane deformation vibrations with PEDs contributions of 10, 25, 16, 58, 29, 15, 17, and 47%, respectively. The modes no. 29, 37, 45, and 48 are described as C–C–C out–of–plane deformation. The C–C–C out–of–plane deformation computed by B3LYP/6–31G (d,p) method also show good agreement with recorded spectral data.

5 Conclusions

In the present study, the l-hydroxy-2-naphthoic acid (1H2NA) in solid phase was completely characterized by using the FT–IR, FT–Raman and UV–Vis spectroscopies. The structural, electronic, UV–Vis analysis and vibrational frequencies of the title compound have been calculated by the DFT/B3LYP/6–31G (d,p) method. In order to take into account the effect of intermolecular interaction, the 1H2NA dimer formed by O–H···O intermolecular hydrogen bonds was investigated by theoretical method. The optimized geometric parameters (bond lengths, bond angles and dihedral angles) of 1H2NA monomer and dimer forms are theoretically determined and compared with the experimental results. On the basis of the agreement between the calculated and observed results, assignments of fundamental vibrational modes of the title compound

were examined based on the results of the PED output obtained from normal coordinate analysis. After scaling down, the calculated wave numbers show good agreement with the FT–IR and FT–Raman spectra. The TD–DFT calculations lead to a very closer agreement with the experimental absorption spectra in ethanol solvent. Nonlinear optical property of the studied compound was investigated by determining the ground-state dipole moment, the mean polarizability, the anisotropy of the polarizability, and the mean first-order hyperpolarizability using the DFT/B3LYP method. So, it is demonstrated that the investigated compound can be used as a NLO material. Moreover, in order to obtain information about the negative and positive regions that are possible sites for the electrophilic and nucleophilic attack, respectively. The 3D molecular surfaces were simulated. A complete vibrational study, accomplished through the analysis of the FT–IR and FT–Raman were also compared with the vibrational spectra, obtained from DFT/B3LYP/6–31G(d,p) level, as a dimer for the first time.

Acknowledgement

The authors would like to thank Kocaeli University Research Fund for its financial support (Grant No. 2017/015HD).

References

1 Talukder M & Kates C R, *Naphthalene Derivatives, In Kirk-Othmer Encyclopedia of Chemical Technology*, Wiley: New York, 2000.
2 Fukumoto H, Oki Y, Kitamura K & Hayashi H, *US Patent Office*, 7 (2006) 669 B2.
3 Karger E, Arfington R & MacGregor P T, *US Patent Office*, 3 (1974) 453.
4 Ji N, Rosen B M & Myers A G, *Org Lett*, 6 (2004) 4551.
5 Krishnakumar V, Mathammal R & Muthunatesan S, *Spectrochim Acta A*, 70 (2008) 201.
6 Zhang Q, Li M & Mei X*, Acta Cryst*, B71 (2015) 119.
7 Frisch M J, *Gaussian 09, Revision A1, Gaussian Inc*, Wallingford, CT, 2009.
8 Keith T & Millam J, *GaussView*, *Version 5.0.9*, Semichem Inc., Shawnee Mission KS, 2009.
9 Becke A D, *J Chem Phys***,** 98 (1993) 5648.
10 Lee C, Yang W & Parr R G, *Phys Rev B***,** 37 (1988) 785.
11 Jamroz M H, *Vibrational Energy Distribition Analysis (VEDA 4)*, Warsaw: Poland, 2004.
12 Koopmans T C, *Physica (Amsterdam)*, 1 (1934) 104.
13 Senet P, *Chem Phys Lett*, 275 (1997) 527.
14 Charanya C, Sampathkrishnan S & Balamurugan N, *J Mol Liq*, 231 (2017) 116.
15 Parr R G, Szentpaly L & Liu S, *J Am Chem Soc*, 121 (1999) 1922.
16 Abraham J P, Sajan D, Joe I H & Jayakumar V S, *Spectrochim Acta A*, 71 (2008) 355.
17 Karamanis P, Pouchan C & Maroulis G, *Phys Rev A*, 77 (2008) 013201.
18 Sağdınç S G & Eşme A, *Spectrochim Acta A*, 75 (2010) 1370.
19 Chandra S, Saleem H, Sundaraganesan N & Sebastian S, *Spectrochim Acta A*, 74 (2009) 704.
20 Allen F H, *Acta Crystallogr B*, 58 (2002) 380.
21 Krishnakumar V, Mathammal R & Muthunatesan S, *Spectrochim Acta A*, 70 (2008) 210.
22 Eşme A & Sağdınç S G, *J Mol Struct*, 1147 (2017) 322.
23 Fleming I, *Frontier Orbitals and Organic Chemical Reactions*, Wiley, London, 1976.
24 Karelson M, Lobanov V S & Katritzky A R, *Chem Rev*, 96 (1996) 1027.
25 Streitwieser J A, *Molecular Orbital Theory for Organic Chemists*, Wiley, New York, 1961.
26 O'Boyle N M, Tenderholt A L & Langer K M, *J Comput Chem*, 29 (2008) 839.
27 Chen M, Waghmare U V, Friend C M & Kaxiras E, *J Chem Phys*, 109 (1998) 6854.
28 Politzer P, Truhlar D G, *Chemical Application of Atomic and Molecular Electrostatic Potentials*, Plenum, New York, 1981.
29 Parr R G & Yang W, *Density Functional Theory of Atoms and Molecules*, Oxford University Press, London, 1989.
30 Mulliken R S, *J Chem Phys*, 23 (1995) 1833.
31 Andraud C, Brotin T, Garcia C, Pelle F, Goldner P, Bigot B & Collet A, *J Am Chem Soc*, 116 (1994) 2094.
32 Snehalatha M, Ravikumar C, Joe I H, Sekar N & Jayakumar V S, *Spectrochim Acta A*, 72 (2009) 654.
33 Glendening E D, Reed A E, Carpenter J E, Weinhold F, *NBO Version 3.1*, University of Wisconsin, TCl, Madison, 1998.
34 Scott A P & Radom L, *J Phys Chem*, 100 (1996) 16502.
35 Karabacak M & Cinar M, *Spectrochim Acta A*, 86 (2012) 590.
36 Jadrijević M, Takać M & Topić D V, *Acta Pharm*, 54 (2004) 177.
37 Karabacak M, Kose E & Kurt M, *J Raman Spectrosc*, 41 (2010) 1085.
38 Varsanyi G, *Vibrational Spectra of Benzene Derivatives*, Academic Press, New York 1969.
39 Vein D L, Colthup N B, Fateley W G & Grasselli J G, *The Handbook of Infrared and Raman Characteristic Frequencies of Organic Molecules*, Academic Press, San Diego, 1991.
40 Demir S, Dinçer M, Korkusuz E & Yildirim I, *J Mol Struct*, 980 (2010) 1.
41 Krishnakumar V, Mathammal R & Muthunatesan S, *Spectrochim Acta A*, 70 (2008) 201.
42 Coates J, *Interpretation of infrared spectra a practical approach*, John Wiley & Sons Ltd, Chichester, 2000.
43 Eşme A & Sağdınç S G, *Acta Phys Pol A*, 130 (2016) 1273.
44 Varsanyi G, *Assignment for Vibrational Spectra of Seven Hundred Benzene Derivatives*, Academic Kiaclo, Budapest, 1973.
45 Socrates G, *Infrared Characteristic Group Frequencies*, Wiley, New York, 1980.
46 Surisseau C & Marvel P, *J Raman Spectrosc*, 25 (1994) 447.
47 Barnes A J, Majid M A, Stuckey M A, Gregory P & Stead C V, *Spectrochim Acta A***,** 41 (1985) 629.